

1 **Determining the water-cement ratio, cement content, water content and degree**
2 **of hydration of hardened cement paste: Method development and validation on**
3 **paste samples**

4 H.S. Wong¹ and N.R. Buenfeld

5 *Concrete Durability Group, Imperial College London, SW7 2AZ, UK*

6
7 **Abstract**

8 We propose a new method to estimate the initial cement content, water content and free water/cement ratio (w/c)
9 of hardened cement-based materials made with Portland cements that have unknown mixture proportions and
10 degree of hydration. This method first quantifies the composition of the hardened cement paste, i.e. the
11 volumetric fractions of capillary pores, hydration products and unreacted cement, using high-resolution field
12 emission scanning electron microscopy (FE-SEM) in the backscattered electron (BSE) mode and image analysis.
13 From the obtained data and the volumetric increase of solids during cement hydration, we compute the initial
14 free water content and cement content, hence the free w/c ratio. The same method can also be used to calculate
15 the degree of hydration. The proposed method has the advantage that it is quantitative and does not require
16 comparison with calibration graphs or reference samples made with the same materials and cured to the same
17 degree of hydration as the tested sample. This paper reports the development, assumptions and limitations of the
18 proposed method, and preliminary results from Portland cement pastes with a range of w/c ratios (0.25-0.50) and
19 curing ages (3-90 days). We also discuss the extension of the technique to mortars and concretes, and samples
20 made with blended cements.

21 Keywords: Backscattered electron imaging (B); image analysis (B); microstructure (B); SEM (B); w/c ratio

22
23 **1. Introduction**

24 The mass ratio of water-to-cement content is one of the most fundamental parameters in concrete mixture
25 proportioning. The w/c ratio has a significant influence on most properties of hardened concrete in particular

¹ Corresponding author: Tel: +44 (0)20 7594 5957; Fax: +44 (0)20 7225 2716

E-mail address: hong.wong@imperial.ac.uk

26 strength and durability [1] due to its relationship with the amount of residual space i.e. capillary porosity, in the
27 cement paste. Since the w/c ratio is an indication of the quality of a concrete mix, the situation often arises where
28 it is desirable to examine the original w/c ratio of a particular concrete some time after it has hardened. This is
29 often carried out in disputes when non-compliance with the mix specification is suspected. Determination of the
30 w/c ratio is also important for quality control during concrete production and general quality assurance purposes.

31

32 Unfortunately, once concrete has set, it is very difficult to ascertain the exact amounts of cement and water that
33 were originally added during batching. There is yet to be a standardised and universally accepted technique for
34 accurately determining the original w/c ratio of a sample taken from an existing structure [2]. BS 1881: Part 124:
35 1988 [3] describes a physico-chemical method to calculate the original w/c ratio by separate estimations of the
36 original cement content from partial chemical analysis (for soluble silica and calcium oxide) and original water
37 content from the sum of chemically bound water and the volume of capillary pores, which in turn, is obtained
38 from vacuum saturation of a dried sample with a liquid of known density. This method cannot be used for
39 concretes that are damaged, either physically or chemically, concretes that are poorly compacted and concretes
40 with entrained air or unusually porous aggregates. This method is also known to have a low precision, estimated
41 to be within 0.1 (w/c ratio, by mass) [4] or even greater [2, 5], and therefore has little practical value.

42

43 Nordtest Build NT 361-1999 [6] describes a method for estimating w/c ratio using fluorescence microscopy. The
44 sample is first impregnated with a resin containing fluorescent dye. A polished thin-section of the sample is then
45 produced and subsequently examined using a petrographic microscope. The intensity of the fluorescence emitted
46 from the cement paste is proportional to the amount of intruded resin, which in turn is related to the capillary
47 porosity and the w/c ratio. Indeed, many studies have confirmed that the change in fluorescence intensity could
48 be related to a change in w/c ratio [5, 7-10]. Hence, if a set of suitable reference standards made of a similar
49 concrete with known w/c ratio is available, one can allocate an equivalent w/c ratio to the sample in question by
50 visual comparison. Sahu et al. [11] proposed another microscopy-based method to estimate the w/c ratio of
51 hardened concrete. Using scanning electron microscopy in the backscattered electron (BSE) mode, the authors
52 measured the capillary porosity thresholded at grey level < 50 at standardised brightness and contrast settings.
53 This was plotted against w/c ratio for a set of reference samples and a good linear correlation was obtained. The

54 equation of the best-fit line was subsequently used to calculate the w/c ratio of unknown samples.

55

56 The main drawback of the current microscopy-based methods is the need to use reference standards for
57 comparison or calibration purposes. In the fluorescence microscopy method, the reference standards need to
58 have the same cement and aggregate type, air void content and degree of hydration, in addition to the w/c ratio,
59 as the concrete being examined [2, 5]. In the electron microscopy method, the reference standards should have
60 the same degree of hydration as the tested sample. For field concretes, the materials used may not be known or
61 available. If the materials are known and available, the curing and exposure history is usually unknown. The
62 curing and exposure history affect the degree of hydration, which influences the capillary porosity and the
63 amount of intruded resin. Therefore, it has been recommended that these techniques be only used for relatively
64 mature Portland cement concrete, but whether this precautionary measure is sufficient or not is debatable.

65

66 In this paper, we propose a new microscopy-based method for estimating the w/c ratio that does not require
67 comparison to any reference standards. We are interested in the ‘free’ w/c ratio, i.e. the amount of water present
68 in the mix at the time of setting excluding any water ‘lost’ to aggregate absorption and evaporation. The free w/c
69 ratio is more relevant than the total w/c ratio for ascertaining concrete quality because the absorbed and
70 evaporated water prior to setting plays no part in the formation of capillary pores. The method is also able to
71 determine the initial free water and cement content, and the degree of hydration of an unknown mix composition.
72 This paper reports the development, assumptions and limitations of the proposed method, and preliminary results
73 from Portland cement pastes with a range of w/c ratios and curing ages. Pastes were chosen for this preliminary
74 study since they can be prepared with well-controlled free w/c ratio. We also discuss the extension of the
75 technique to mortars and concretes, and samples made with blended cements.

76

77 **2. Proposed method**

78 *2.1 Theoretical development*

79 The chemistry of Portland cement hydration is complex and not fully understood, although much progress has
80 been made over the years. In the simplest representation, cement reacts with water to form products of hydration,

81 which precipitate out from a saturated solution to form solids. The hydration products consist of crystalline (CH,
 82 AFt, AFm) among others and non-crystalline (C-S-H gel) phases having different physical and chemical
 83 properties, but for simplicity, they will be considered collectively as a single component in this paper. The solid
 84 hydration products occupy a greater volume than the volume of the reacted cement, but slightly smaller than the
 85 sum of the volumes of the cement and water due to chemical shrinkage. As a result of the increase in the total
 86 solids volume, the originally water-filled spaces (capillary pores) become progressively filled with time.

87

88 At any moment after setting, the hardened cement paste can be thought to consist of four main components: a)
 89 the remaining unreacted cement; b) the crystalline and semi-crystalline hydration products, including their
 90 intrinsic ‘gel pores’; c) the capillary pores and d) air voids from incomplete compaction and deliberate
 91 entrainment. This is schematically represented in Figure 1. The sum of the absolute volumes of these four
 92 components and any shrinkage must be equal to the total volumes of the original cement content, free water and
 93 air voids at the time of set. The total shrinkage is small and negligible for the purpose of this investigation (see
 94 Discussion). We assume that the volume of entrapped and entrained air is invariant with time since the hydration
 95 products are expected to occupy the water-filled capillary pores only. Therefore, at any hydration degree, we can
 96 write:

$$97 \quad V_C + V_W = V_{AH} + V_{HP} + V_{CP} \quad (1)$$

98 Where V_C , V_W , V_{AH} , V_{HP} and V_{CP} represent absolute volumes of the original cement, original free water,
 99 unreacted (anhydrous) cement, hydration products and capillary pores. Next, we consider the volumetric ratio of
 100 hydration products to the reacted cement, which we call δ_V in this paper. It is well known that for any room
 101 temperature cured contemporary Portland cements at any w/c ratio and age, the cement hydration products
 102 occupy approximately twice the volume of reacted cement, i.e. $\delta_V \sim 2$. The actual value of δ_V is slightly
 103 dependent on the cement composition (shown later), and typical values of between 2.1 and 2.2 have been
 104 reported in the literature [1, 12, 13]. Thus:

$$105 \quad V_C = V_{AH} + \frac{V_{HP}}{\delta_V} \quad (2)$$

$$106 \quad \text{And from (1):} \quad V_W = V_{AH} + V_{HP} + V_{CP} - \left(V_{AH} + \frac{V_{HP}}{\delta_V} \right) = V_{HP} \left(1 - \frac{1}{\delta_V} \right) + V_{CP} \quad (3)$$

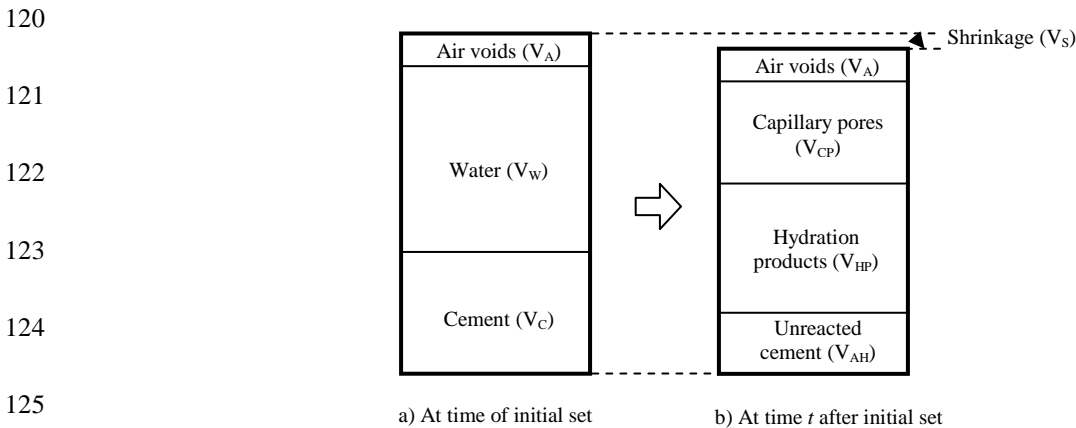
107 Therefore, if the specific gravity of cement is ρ_c , we can express the free w/c ratio as:

108
$$\frac{w}{c} = \frac{V_W}{V_C \times \rho_c} = \frac{V_{HP}(\delta_V - 1) + \delta_V V_{CP}}{(\delta_V V_{AH} + V_{HP})\rho_c} \quad (4)$$

109 The degree of hydration (m) can be estimated from the fraction of cement reacted. By substituting V_c with Eq. 2,
110 we can express the degree of hydration as:

111
$$m = \frac{V_C - V_{AH}}{V_C} = \frac{V_{HP}}{\delta_V V_{AH} + V_{HP}} \quad (5)$$

112 Thus, it appears that the original cement content, free water content, free w/c ratio and the degree of hydration
113 can be determined, at any time after setting, from the volumetric ratio of hydration products to the reacted
114 cement δ_V and the volumetric fractions of the unreacted cement, hydration products and capillary pores at the
115 time of test. The latter may be directly measured using microscopy and image analysis techniques. The
116 application of the method does not require prior knowledge of the original cement content and is not affected by
117 curing age; hence it may be suitable for testing field samples. However, the method will require: 1) a precise
118 description of δ_V , 2) the ability to image the capillary pores, hydration products and unreacted cement, and 3) an
119 accurate and reproducible image analysis routine to segment and quantify these.



126 **Figure 1: Schematic representation of the volumetric proportions of the main components in hardened**
127 **cement paste at time of initial set (a) and at time t after setting (b).**

128

129 **2.2 Derivation of δ_V from Powers and Brownyard's model**

130 As stated earlier, a good first approximation for δ_V is 2 since Portland cements form hydration products that
131 occupy about twice the volume of reacted cement at any w/c ratio and age. The actual value of δ_V , however, is

132 slightly dependent on the cement composition and this can be derived from the work of Powers and Brownyard
 133 [14]. In Powers and Brownyard [14] proposed that water in cement paste can be classified as evaporable
 134 (capillary and gel water) and non-evaporable (chemically bound water). The gel water is the water adsorbed by
 135 the fine nanoscale characteristic pores in the hydration products. Accordingly, the volume of the hydration
 136 products (V_{HP}) and reacted cement ($V_{C'}$) can be written as:

$$137 \quad V_{HP} = c'v_c + w_n v_n + w_g v_g \quad \text{and} \quad V_{C'} = m c' v_c \quad (6)$$

138 Where c' , w_n and w_g are the mass of the reacted cement, non-evaporable water and gel water respectively, and v_c ,
 139 v_n and v_g are the specific volumes of the cement, non-evaporable water and gel water respectively. The
 140 volumetric ratio of hydration products to the reacted cement δ_V is thus:

$$141 \quad \delta_V = \frac{V_{HP}}{V_{C'}} = \frac{c'v_c + w_n v_n + w_g v_g}{m c' v_c} = 1 + \frac{w_n}{c'} \frac{v_n}{v_c} + \frac{w_g}{c'} \frac{v_g}{v_c} \quad (7)$$

142

143 To apply Equation 7, the functions w_n/c' and w_g/c' , which are the non-evaporable water per mass of hydrated
 144 cement and the gel water per mass of hydrated cement respectively, and the specific volumes of the non-
 145 evaporable water and gel water, need to be known. Powers and Brownyard [14] performed numerous
 146 experiments on neat cement pastes and mortars made with 86 types of cement (commercial and laboratory
 147 prepared) of different compositions at various w/c ratios (0.31-0.61) and curing ages (7-479 days) and found that
 148 these functions are relatively constant, and only slightly dependent on the cement composition. This is a crucial
 149 finding because it suggests that all Portland cements hydrate at room temperature to form approximately the
 150 same hydration products, at approximately the same rate and mutual proportions [15, 16].

151

152 Powers and Brownyard [14] determined the non evaporable water content (w_n) by ignition to 1000°C following
 153 P-drying (in an evacuated desiccator over $Mg(ClO_4)_2 \cdot 2H_2O$ until constant mass), which removed the evaporable
 154 water first. They observed that w_n mainly depended on the amount of reacted cement and the ratio w_n/c' can be
 155 approximated as a function of the clinker mineral composition:

$$156 \quad \frac{w_n}{c'} = 0.187x_{C_3S} + 0.158x_{C_2S} + 0.665x_{C_3A} + 0.213x_{C_4AF} \quad (8)$$

157 Where x represent the mass fractions of the C_3S (alite), C_2S (belite), C_3A (aluminat) and ferrite (C_4AF). To
 158 obtain the gel water content, Powers and Brownyard [14] then performed water vapour sorption experiments on
 159 the P-dried samples and found that the amount of water held at RH below 45% is proportional to the amount of
 160 cement reacted, and thus to the gel pore volume, and that at RH greater than 45%, the water condenses in the
 161 larger capillary pores. Applying B.E.T. theory to the measured adsorption isotherm, Powers and Brownyard [14]
 162 then introduced and measured the property V_m/w_n , where V_m corresponds to the mass of water to cover the
 163 hydration products with a single monolayer of water, this being achieved at RH of about 20%. Thus, the ratio
 164 V_m/w_n represents the specific internal surface and again, they found that this is relatively constant with w/c ratio
 165 and curing age, but depends on the cement composition. The following empirical fit was obtained:

$$166 \quad \frac{V_m}{w_n} = 0.230x_{C_3S} + 0.320x_{C_2S} + 0.317x_{C_3A} + 0.368x_{C_4AF} \quad (9)$$

167 Powers and Brownyard [14] further observed that the maximum amount of water that can be retained by the
 168 hydration product, i.e. gel water, corresponds to $4V_m$. Therefore, the parameter w_g/c' in Equation 7 can be
 169 obtained by multiplying the experimentally derived w_n/c' (Equation 8) and $4V_m/w_n$ (Equation 9). The non-
 170 evaporable water and gel water were considered to be 'compressed' i.e. having specific volumes (v_n and v_g
 171 respectively) lower than that of the free water ($= 1\text{cm}^3/\text{g}$). Using a pycnometer and helium displacement
 172 measurements on P-dried samples, it was found that the specific volume of non-evaporable water (v_n) did not
 173 vary much for all examined pastes and that the value of $0.72\text{cm}^3/\text{g}$ was representative [16]. Subsequently, the
 174 specific volume of gel water (v_g) could be determined indirectly as $0.90\text{cm}^3/\text{g}$.

175

176 Powers and Brownyard's [14] classification of water in cement paste is somewhat arbitrary since an overlap in
 177 binding energies of the water phases is expected, but their model allows quantitative calculation of the cement
 178 paste composition and explains many different properties of the cement paste [15, 19]. Although the accuracy
 179 with which the non-evaporable water and gel water can be separately measured is questionable, the sum of the
 180 non-evaporable and gel water content is useful and remains relevant to this study. Some of the gel water or even
 181 the non-evaporable water is probably removed during drying when measuring capillary porosity. However, a
 182 similar condition occurs in samples prepared for electron microscopy, and thus the value δ_v is transferable to this
 183 technique.

184

185 3. Experimental

186 3.1 Materials and sample preparation

187 Five ordinary Portland cement pastes with w/c ratios 0.25, 0.30, 0.35, 0.40 and 0.50 were prepared using cement
188 complying with BSEN197-1-CEM 1 and tap water. The cement has a Blaine specific surface area and specific
189 gravity of 342m²/kg and 3.15 respectively. Its mineral composition, calculated from the modified form of the
190 Bogue calculation [21], is 63% alite, 12.8% belite, 7.4% aluminate and 8.3% ferrite. Therefore, using Equations
191 7-9, its δ_v is 2.02.

192

193 The mixing was done using a bowl mixer and the samples were compacted in two equal layers into plastic
194 cylindrical moulds (58mm diameter, 49mm height) using a vibrating table with adjustable intensity. For each
195 layer, compaction was assumed complete when no significant amount of air bubbles escaped the surface. The
196 samples were then capped and sealed, taking care to minimise any entrapped air. Subsequently, they were rotated
197 slowly for 24 hours to avoid bleeding and segregation effects.

198

199 After the initial 24 hours, the samples still in their plastic containers, were wrapped in cling film and sealed in
200 polythene bags at 20°C until the ages of 3, 7, 28 and 90 days. At the end of each curing age, one cylinder was
201 sectioned at mid-height using a diamond saw to produce a rectangular block sample (40 x 20 x 8mm) for
202 microscopy. The block samples were freeze-dried to remove the pore water and then impregnated with low
203 viscosity epoxy (pre-heated to 50°C and thinned with toluene) using the methodology described by Wong &
204 Buenfeld [22]. It is critical to ensure that the blocks are properly impregnated with epoxy to preserve the delicate
205 microstructure and to provide atomic contrast to the capillary pores. The epoxy impregnated blocks were cured
206 for several days at room temperature to allow proper hardening of the epoxy. Following this, they were ground
207 and polished with diamond in the usual manner at successively finer grades to a ¼-micron finish.

208

209 3.2 BSE imaging

210 The volume fractions of unreacted cement, hydration products and capillary pores were measured by image

211 analysis on backscattered electron (BSE) images [19]. A Camscan Apollo 300 FE-SEM was used for BSE
212 imaging. The FE-SEM gives a better resolving power than conventional SEM because the brighter and more
213 stable electron source is able to produce a higher density beam, but at smaller beam size and at lower energy
214 [20]. Prior to imaging, the brightness and contrast settings of the microscope were calibrated so that the
215 brightness histogram of the recorded image was centred and stretched to span the entire dynamic range of the
216 available grey scale (0 to 255) for each image. This required a trial and error approach, but once the optimum
217 brightness and contrast setting had been found, the same setting was applied to all subsequent images. This is
218 important to ensure a faithful reproduction of grey values in every image over the entire range of samples
219 investigated so that a meaningful comparison and accurate quantitative data can be obtained.

220

221 Imaging was performed at low vacuum (40Pa), so no sample coating was necessary to avoid charging effects.
222 Thirty images were collected randomly for each sample by programming the stage to move in a grid fashion and
223 stopping at predefined, equally spaced co-ordinates, spanning the entire sample surface. This provided a
224 systematic sampling approach to ensure that sampling was random and uniform. The images were captured at
225 10kV accelerating voltage, 10mm working distance and 500x magnification. The images were digitised to 2560
226 x 2048 pixels at a pixel spacing of 0.094 μ m, giving an image field of view of 240 x 192 μ m. This magnification
227 and pixel spacing level was chosen as a compromise to obtain adequate resolution and a representative sampling
228 area.

229

230 **3.3 Image analysis**

231 The unreacted cement, hydration products and capillary pores are segmented from the BSE images to allow
232 measurement of their area and volumetric fractions using stereology [23]. Segmentation is the first step in
233 quantitative image analysis and also the most crucial because all subsequent measurements are carried out on the
234 segmented image. An appropriate thresholding method must be employed so that the results are accurate and
235 reproducible. However, segmentation of a digital image can never be error free due to various reasons such as
236 the finite-pixel size effect and the overlapping of signal sampling volumes. Nevertheless, these errors can be
237 reduced by using an objective and consistent thresholding rule.

238

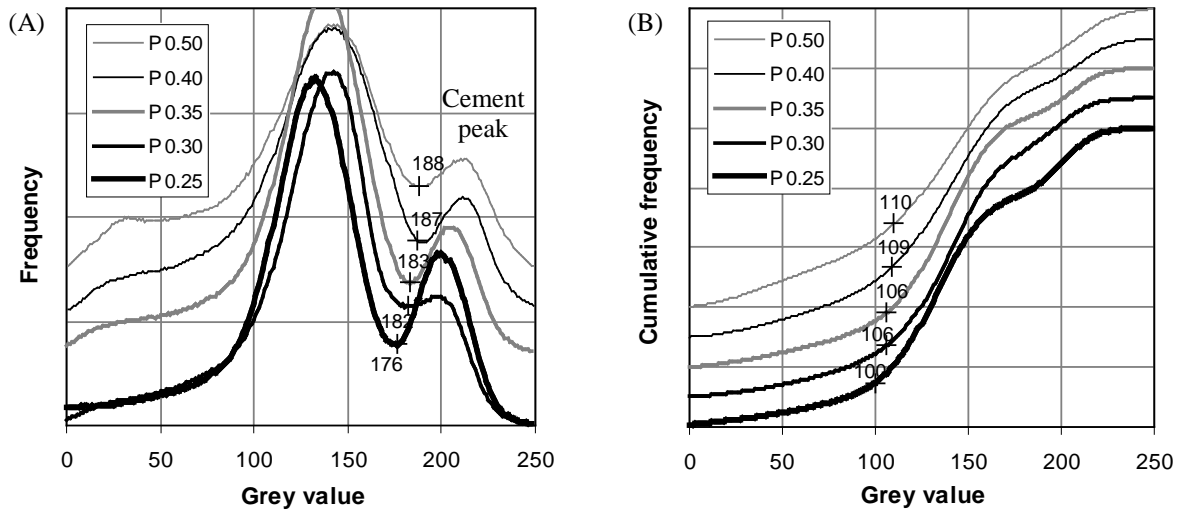
239 The unreacted cement particles are highly contrasted from the hydration products so segmentation is relatively
240 easy by selecting the minimum grey value between peaks for hydration products and the unreacted cement as the
241 lower threshold value (Figure 2A). The exact location of the minima is determined from the first derivative of
242 the brightness histogram. The capillary pores are segmented using the 'overflow' method proposed by Wong et
243 al. [24], whereby the inflection point of the cumulative brightness histogram is taken as the upper threshold
244 value. This is obtained from the intersection of two best-fit lines in the cumulative brightness histogram. For the
245 purpose of this study, the capillary porosity is considered to include the hollow shell pores since Powers and
246 Brownyard's model does not distinguish the latter pore type. Microcracks due to damage caused by the sample
247 preparation should not be included and care was taken to avoid imaging these areas, in particular near the sample
248 edges. Nevertheless, the amount of microcracking observed in the samples was small and therefore considered
249 not to have a significant influence.

250

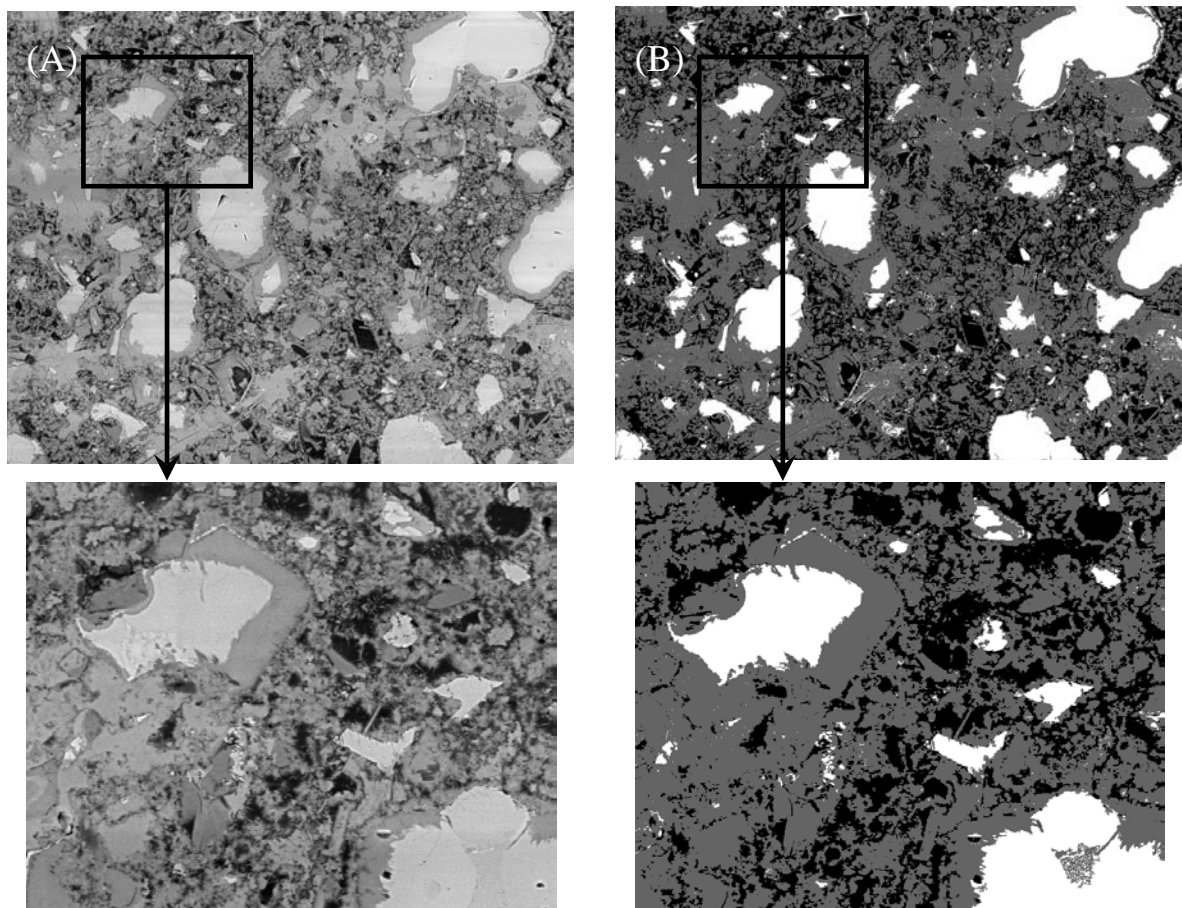
251 Figures 2A and 2B show examples of the obtained thresholds for unreacted cement and capillary pores, selected
252 from the range of samples investigated. Note that the histograms are vertically offset to improve clarity. The
253 absolute threshold values are not constant, but vary slightly due to small (and unavoidable) fluctuations of the
254 beam conditions, chamber pressure or specimen surface conditions. Nevertheless, since every image is
255 thresholded using consistent rules, the effect of this on the measured volumetric fraction is small. Finally, the
256 volume fraction of hydration products is obtained by simple subtraction, taking care to exclude any entrapped air
257 voids, which can be easily distinguished due to their large size and spherical shape.

258

259 Figure 3 shows an example of the original BSE image and the segmented image, highlighting the effectiveness
260 of the segmentation procedure. The volume fractions obtained from each frame are then used to calculate the
261 'local' cement content, free water content, free w/c ratio and degree of hydration, using Equations 2 to 5. This is
262 repeated for a large number of frames (typically 30 images are required) until their cumulative averages from
263 successive frames do not vary significantly, thereby indicating that a representative volume has been analysed.



264 **Figure 2: Segmentation of the unreacted cement and capillary pores. The threshold (marked as +) for**
 265 **unreacted cement is selected from the minimum between peaks for hydration products and unreacted**
 266 **cement on the brightness histogram (A). The threshold for porosity is obtained from the inflection point of**
 267 **the cumulative brightness histogram (B).**
 268



269
 270
 271
 272
 273
 274
 275
 276
 277
 278
 279
 280
 281
 282
 283
 284
 285
 286
 287
 288
 289 **Figure 3: Comparison between an original BSE image (A) and the segmented image (B) for measuring the**
 290 **volume fractions of the unreacted cement (white pixels), hydration products (dark grey pixels) and**
 291 **capillary pores (black pixels). Insets show magnified portions of the original images, highlighting the**
 292 **effectiveness of the segmentation procedure. Sample is a w/c 0.4 paste cured for 3 days. Field of view is 240**
 293 **x 192µm (67 x 54µm for insets).**

294

295 **3.4 Degree of hydration**

296 The degree of hydration was estimated using the proposed method (Equation 5) and the results compared to the
 297 conventional method of measuring the non-evaporable water content by loss-on-ignition (LOI). At the end of
 298 each curing age, the remaining pieces (~35g) from each cylindrical sample were dried in an oven at 105°C until
 299 constant mass to remove all evaporable water, then crushed and heated to 1050°C for 3 hours. The non-
 300 evaporable water was taken as the mass loss between 105°C and 1050°C, corrected for the LOI of the dry
 301 cement powder (=1.36%). The degree of hydration, $m(LOI)$, was then calculated as the ratio of the non-
 302 evaporable water content per gram cement to the amount at complete hydration, which is assumed to be equal to
 303 0.23g/g for OPC.

304

305 The degree of hydration was also estimated by using a conventional image analysis method that first measures
 306 the volume fraction of the unreacted cement (V_{AH}) from BSE images. If the original cement content of the
 307 sample (V_C) is known a priori, then the degree of hydration, $m(IA)$, can be calculated as:

$$308 \quad m(IA) = 1 - \frac{V_{AH}}{V_C} \quad (10)$$

309 Note that our proposed method (Equation 5), in contrast to the conventional image analysis method (Equation
 310 10), does not require prior knowledge of the original cement content.

311

312 **4. Results**

313 The average volume fractions of unreacted cement, hydration products and capillary porosity measured from
 314 image analysis and the average degree of hydration measured from the non-evaporable water content for all
 315 samples are given in Table 1. As expected, samples with lower w/c ratios have higher unreacted cement content
 316 and lower capillary porosity. The degree of hydration from LOI for all w/c ratios and curing ages ranged
 317 between 0.48 and 0.88. For samples at the same w/c ratio, the unreacted cement content and detectable capillary
 318 porosity decreases with an increase in hydration degree.

319

320 **Table 1: Measured volume fractions of unreacted cement, hydration products and capillary porosity from**
 321 **image analysis (average of 30 frames at each age), estimated w/c and the degree of hydration from loss-on-**
 322 **ignition. Values in parentheses represent the respective standard errors.**

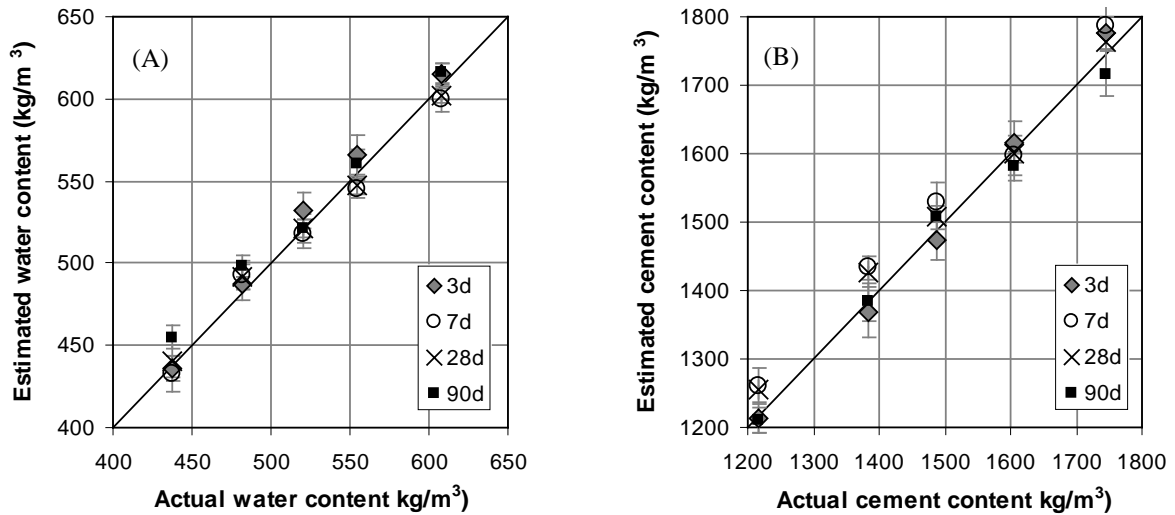
Sample	Unreacted cement (%)				Hydration products (%)				Porosity (%)				Estimated w/c				Hydration degree m (LOI)			
	3d	7d	28d	90d	3d	7d	28d	90d	3d	7d	28d	90d	3d	7d	28d	90d	3d	7d	28d	90d
P 0.50	14.8 (0.5)	11.0 (0.5)	7.8 (0.4)	6.1 (0.4)	47.9 (0.6)	58.6 (0.6)	64.7 (0.6)	65.2 (0.5)	37.3 (0.4)	30.4 (0.5)	27.5 (0.4)	28.6 (0.4)	0.51 (0.007)	0.48 (0.007)	0.48 (0.004)	0.51 (0.005)	0.69	0.70	0.77	0.88
P 0.40	15.8 (0.8)	14.4 (0.5)	10.5 (0.5)	10.1 (0.5)	55.9 (0.7)	62.8 (0.6)	70.2 (0.6)	68.2 (0.9)	28.4 (0.6)	22.8 (0.4)	19.3 (0.3)	21.6 (0.7)	0.42 (0.009)	0.38 (0.004)	0.38 (0.004)	0.41 (0.007)	0.64	0.67	0.72	0.87
P 0.35	17.4 (0.5)	18.11 (0.8)	14.6 (0.7)	13.3 (0.6)	59.4 (0.4)	61.4 (0.9)	67.3 (0.6)	69.7 (0.7)	23.3 (0.4)	20.5 (0.5)	18.1 (0.3)	17.0 (0.3)	0.36 (0.005)	0.34 (0.005)	0.35 (0.005)	0.35 (0.004)	0.59	0.61	0.73	0.80
P 0.30	23.5 (0.7)	21.6 (0.6)	17.2 (0.5)	16.2 (0.6)	56.2 (0.6)	58.9 (0.7)	67.8 (0.5)	68.6 (0.7)	20.3 (0.4)	19.5 (0.5)	14.9 (0.3)	15.1 (0.2)	0.30 (0.005)	0.31 (0.005)	0.31 (0.004)	0.32 (0.004)	0.54	0.58	0.66	0.69
P 0.25	27.9 (0.7)	27.8 (0.9)	25.2 (0.8)	22.6 (0.7)	57.5 (0.7)	58.5 (0.8)	62.2 (0.6)	64.4 (0.8)	14.6 (0.3)	13.8 (0.3)	12.6 (0.3)	13.0 (0.3)	0.25 (0.004)	0.24 (0.005)	0.25 (0.005)	0.27 (0.004)	0.48	0.49	0.57	0.62

323

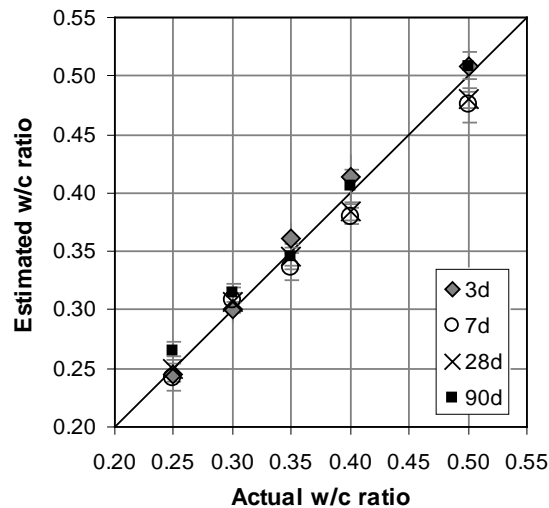
324 Taking δ_V equal to 2.02 and the specific gravity of cement as 3.15, the original cement content, water content and
 325 free w/c ratio are calculated using Equations 2 to 4. The results are plotted against their actual values in Figures 4
 326 and 5. The y-axis error bars for each data point indicate the 95% confidence interval calculated using Student's t-
 327 distribution.

328

329 The local variation in w/c ratio is indicated more clearly in the frequency distribution histograms shown in
 330 Figure 6. For instance, for the paste samples cast with original w/c ratio of 0.35, the estimated w/c ratio at each
 331 image location (representing an area of 240 x 192 μm) for all 120 images was found to range from 0.25 to 0.45.
 332 This apparently large range in the local w/c ratio is not surprising because cement-based materials are known to
 333 be heterogeneous at the micro-scale. The observed variability also depends on the field of view, and is expected
 334 to increase with smaller imaged area, which is a trade-off for better resolution. Nevertheless, when a
 335 representative number of frames are measured and averaged, there appears to be a generally good agreement
 336 between the estimated and the actual values for the water content, cement content and w/c ratio across all
 337 samples and curing ages investigated (Figures 4 and 5). As mentioned in Section 3.3, the number of images
 338 required for a representative measurement can be determined from a plot of cumulative averages with successive
 339 frames analysed.



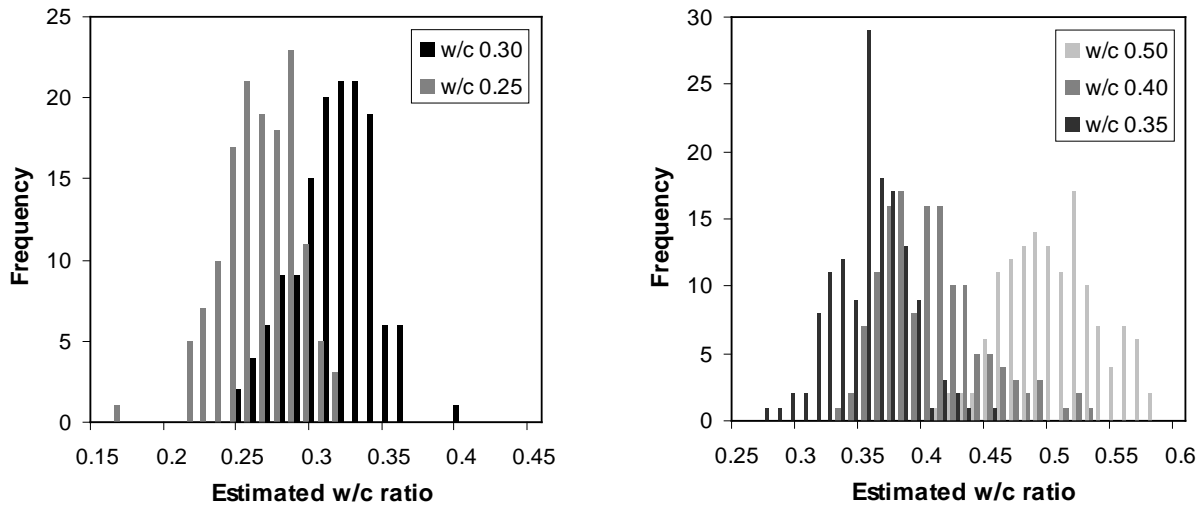
340 **Figure 4: Comparison between the estimated and actual values of the original water content (A) and**
 341 **cement content (B) for all samples investigated. The error bars represent 95% confidence interval.**
 342



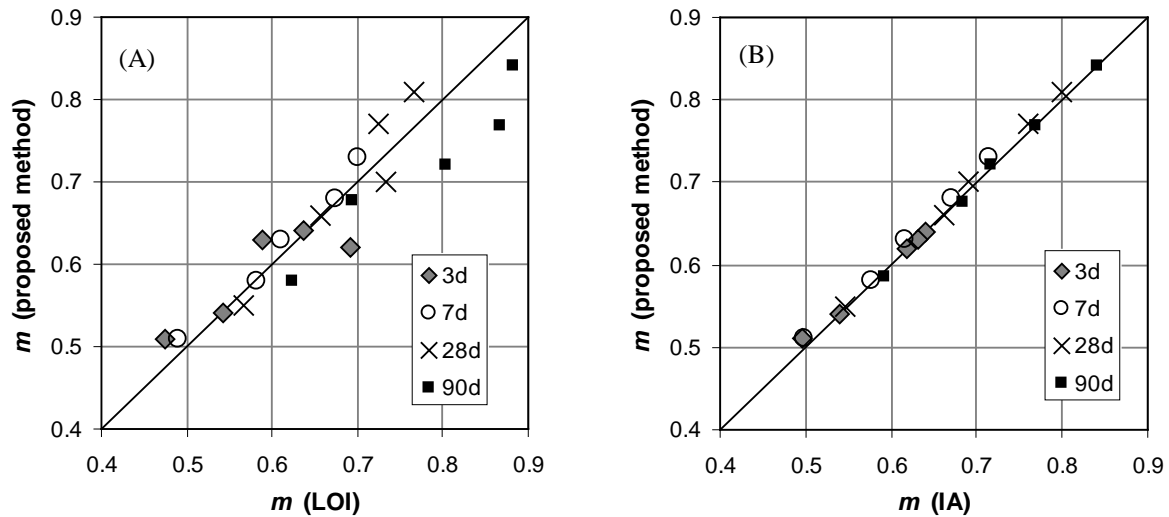
343 **Figure 5: Comparison between the estimated and actual values of the water-cement ratio for all samples**
 344 **investigated. The error bars represent 95% confidence interval.**
 345

346 In Figure 7, the estimated degree of hydration is compared against the measured values from the LOI test (Fig.
 347 8a) and conventional image analysis (Fig. 8b). Again, a relatively good agreement between the estimated and
 348 measured values is observed for both cases. It is interesting to note that the correlation with the conventional
 349 image analysis method is slightly better when compared to the LOI method. This suggests that some errors may

350 stem from the LOI test such as 1) dehydration of the C-S-H, AFm and Aft phases may have occurred at
 351 temperatures below 105°C, making the LOI results lower than actual values, and 2) the mass loss between 105C
 352 and 1050°C may also be due to the decomposition of other volatile phases, such as carbonates, which would
 353 make the LOI results higher than actual values.



354 **Figure 6: Frequency distribution histograms indicating a significant spatial variation in the ‘local’ w/c**
 355 **ratio. Each histogram plot is obtained from 120 data points (30 frames per sample per curing age)**
 356



357 **Figure 7 Comparison between the estimated degree of hydration using the proposed method (Eq. 5) and**
 358 **the measured degree of hydration from a) loss-on-ignition and, b) conventional image analysis method**
 359 **(Eq. 10).**

360

361 The errors in estimating the original cement content, water content and the free w/c ratio ranged from -30 to
 362 +50kg/m³ (-1.7 to +3.7%), -9 to +18 kg/m³ (-1.6 to +4.1%) and -0.025 to +0.015 (-5 to +6%) respectively. For
 363 degree of hydration, the percentage estimation errors ranged from -11.3 to +7.2% and -2.0 to +2.7% when
 364 comparing to the LOI method and conventional image analysis method respectively. It is interesting to note that
 365 the agreement of within $\pm 10\%$ from the LOI method is similar to the results obtained by Feng et al. [25], who
 366 used an SEM point-counting technique for estimating hydration degree. The magnitude of error for all
 367 estimations does not appear to be influenced by either w/c ratio or curing age.

368

369 As expected, the proposed method is sensitive to δ_V . For example, by using a δ_V value of 2.2 instead of 2.02 (i.e.
 370 ~9% increase in δ_V), the range of percentage estimation error for w/c ratio increases to +5 to +14.3%. Therefore,
 371 the δ_V value must be accurately determined for a particular cement composition and the experimental results
 372 from Powers and Brownyard [14] can be used for this purpose (Section 2.2). We have analysed about 170 values
 373 taken from Powers and Brownyard [14] (Tables 2-7, p. 596-601 of Ref. 14) for pastes and mortars prepared from
 374 the 86 cement types representing a wide variation in composition (C₃S: 23-63%; C₂S: 9.3-56%; C₃A: 1.2-15%;
 375 C₄AF: 5.5-22%, from Table A2, p.305-307 of Ref. 14), w/c ratio (0.31-0.61) and curing age (7-479 days).
 376 Considering such a wide range of samples, the calculated δ_V from the original data varied only between 1.8 and
 377 2.3, with mean and median values of 2.13 and 2.15 respectively. However, many cements tested by Powers and
 378 Brownyard [14] have a relatively low C₃S content, unlike contemporary Portland cements. Nevertheless, Powers
 379 & Brownyard [14] also tested cements with high C₃S contents, for example cements 13753, 14560, 15498,
 380 15758, 15924 and 15925 (with C₃S: 60-63%; C₂S: 12-17%; C₃A: 4-11%, C₄AF: 8-14%) and samples made with
 381 these have a calculated δ_V of 2.0-2.1, which is close to the value used in this study.

382

383 5. Discussion

384 The preliminary results show that the proposed method is applicable to ordinary Portland cement pastes with a
 385 range of w/c ratio (0.25 to 0.50) and curing ages (3 to 90 days) and we expect that the method to be extendable to
 386 Portland cement mortars and concretes as well. The presence of aggregates does not influence the model because
 387 their volume fraction is constant with time therefore Equation 1 holds. However, aggregates will increase the
 388 paste heterogeneity due to wall-effect and micro-bleeding causing the interfacial transition zone phenomena,

389 hence more images may need to be captured and analysed to obtain representative results.

390

391 The advantage of the proposed method is that it is able to make separate estimations of the original cement and
 392 water content, which is then used to determine the original w/c ratio. This can be carried out without referring to
 393 calibration or reference standards, or having prior knowledge of the mix proportions. The method also does not
 394 appear to be influenced by hydration degree and curing age. Another advantage of the proposed method is that it
 395 can determine the hydration degree of samples with unknown cement content and samples with aggregates, such
 396 as mortars and concretes. Measurement of hydration degree of mortars and concretes using the LOI technique is
 397 difficult because the aggregates must first be separated from the paste, so that the original cement content can be
 398 obtained from the mass remaining at the end of ignition. The aggregates can be isolated by either crushing
 399 followed by sieving, or by dissolving the paste with concentrated acid, but both methods are known to be not
 400 very effective. As such, the hydration degree of mortars and concretes are often determined from LOI of parallel
 401 cement pastes that have undergone the same curing regime, but the accuracy of this is also questionable.

402

403 In Equation 1, we have assumed that the total shrinkage is small and negligible for the purpose of w/c ratio
 404 estimation. If drying shrinkage is considered, then the formula for w/c ratio, derived following the same principle
 405 can be written as:

$$406 \quad \frac{w}{c} = \frac{(V_{HP} + V_s)(\delta_v - 1) + \delta_v V_{CP}}{(\delta_v V_{AH} + V_{HP} + V_s)\rho_c} \quad (11)$$

407 Where V_s is the change in volume of the hydration products due to loss of adsorbed water, which in theory, can
 408 be approximated as the loss of a water layer of one molecule thick from the surface of all gel particles [1]. Since
 409 the thickness of a water molecule is about 1% of the gel particle size, upon complete drying, a linear change in
 410 dimension from shrinkage (ϵ_s) is expected to be of the order of 10^4 microstrain. In practice, values of up to 4×10^3
 411 microstrain have been observed in pastes [1]. Taking the upper bound value of $\epsilon_s = 10^4$ microstrain, the total
 412 amount of shrinkage (V_s) is only 0.1%, which translates to a difference in the estimated w/c ratio (from
 413 Equations 4 and 11) of no more than 0.0005 for all the samples investigated.

414

415 As in the case of the other techniques currently available for estimating w/c ratio, the proposed method can only
416 be applied to samples that are sound and in no way damaged, either physically or chemically. The samples must
417 not have experienced substantial volumetric change, either excessive shrinkage or expansive reaction such that
418 Equation 1 no longer applies, and reactions that may affect the porosity (e.g. carbonation and leaching) or
419 change the characteristics of the hydration products formed. However, the proposed method may be applicable to
420 concretes that are poorly compacted and with entrained air by carefully excluding the volume fractions of air
421 voids during image analysis. The method is also not affected by bleeding or absorption into porous aggregates as
422 it calculates the free w/c ratio. Samples with excessive bleeding will show a larger spread in the local w/c ratio,
423 therefore requiring more images to be averaged to obtain accurate results.

424

425 The image resolution used in this study may not be sufficient to characterise the entire range of capillary pores,
426 in particular those finer than the pixel spacing ($\sim 0.1\mu\text{m}$). At present, pores finer than the pixel spacing are
427 considered as part of the hydration products. As mentioned earlier, this pixel spacing was chosen as a
428 compromise between achieving adequate sampling size and resolution. The sample can be analysed at a higher
429 magnification and resolution, but because of the smaller field of view, this will come at a cost of increased effort
430 and time since substantially more images must be processed for statistical significance. In addition, image
431 segmentation is never a perfect, error free procedure. Nevertheless, the image digitisation and segmentation can
432 be viewed as an averaging process and small errors from segmentation and finite resolution may actually not
433 have a significant effect on the final result. However, the accuracy of the method when used on data derived
434 from a conventional tungsten filament SEM is unknown. Additional work is needed to study the effect of image
435 magnification and resolution on the accuracy of the proposed method.

436

437 In practice, samples with high w/c ratio (>0.5) will be of most interest in the context of resolving disputes due to
438 suspected non-compliance with the mix specification. Unfortunately, the current study is limited to an upper w/c
439 ratio of 0.5. This was because of difficulties in avoiding segregation during preparation of paste samples that
440 have very high w/c ratio. However, our future study will include mortars and concretes samples with w/c ratio
441 greater than 0.5. Samples with high w/c ratio will have a greater fraction of larger capillary pores, and therefore
442 this reduces the error caused by finite resolution of the imaging system.

443

444 Supplementary cementitious materials are increasingly being utilised in modern concretes. At present, we have
445 not included supplementary cementitious materials in the model, so this will be another major focus of our future
446 work. Clearly, application of the method to samples with binders other than Portland cement will require special
447 considerations. The overall principle of the method appears to be sound as long as an appropriate δ_V is specified
448 according to the cement type, but certain assumptions, for instance the constancy of δ_V with w/c ratio, curing age
449 and exposure needs to be re-examined for these materials. The accuracy of δ_V derived from Powers and
450 Brownyard's model warrants further examination, and this approach may be refined in future studies. Clearly
451 more work is needed to assess how robust the proposed method is when applied to a larger range of cement-
452 based materials, including field samples and various processing and curing methods.

453

454 **6. Conclusion**

455 In this paper, we proposed a new microscopy-based method for estimating the cement content, water content and
456 free w/c ratio of Portland cement-based materials with unknown mixture proportions and degree of hydration.
457 The method first measures the volume fractions of the unreacted cement, hydration products and capillary pores
458 using field emission scanning electron microscopy in the backscatter mode, then calculates the original cement
459 content, free water content and free w/c ratio. The same method can also be used to calculate the degree of
460 hydration. The proposed method makes use of the volumetric ratio of hydration products to the reacted cement
461 (δ_V), which is known from previous studies to be slightly dependent on the cement composition, but invariant to
462 w/c ratio and curing age. This method has the advantage that it is quantitative, and does not require comparison
463 with reference samples made with the same materials and cured to the same hydration degree as the tested
464 sample. Preliminary results are encouraging, whereby a good agreement was observed between the estimated
465 and actual values for ordinary Portland cement pastes with a range of w/c ratios (0.25-0.50) and curing ages (3-
466 90 days). The error in determination for the w/c ratio was no more than 0.025. Future studies will aim to extend
467 the application of the proposed method to blended cements, mortars and concretes.

468

469 **Acknowledgements**

470 HSW acknowledges the support provided by the EPSRC Platform Grant for the Concrete Durability Group
471 (EPSRC GR/M97206). We thank the Reviewers for their constructive comments and suggestions.

472

473 **References**

- 474 [1] Neville, A.M. (1995), *Properties of Concrete*, Fourth Edition, Addison Wesley Longman Ltd.
- 475 [2] Neville, A.M. (2003), How closely can we determine the water-cement ratio of hardened concrete,
476 *Materials and Structures*, Vol. 36, 311-318.
- 477 [3] BS 1881: Part 124: 1988, *Methods for analysis of hardened concrete*, British Standards Institution.
- 478 [4] Concrete Society (1989), *Analysis of hardened concrete*, Technical Report 32, 110.
- 479 [5] St. John, D.A., Poole, A.W., Sims, I. (1998), *Concrete petrography*, Arnold and John Wiley & Sons,
480 London, 474pp.
- 481 [6] NT Build 361-1999, *Concrete, hardened: water-cement ratio*, Nordtest Method, Edition 2, 1999.
- 482 [7] Christensen, P., Gudmundsson, H., Thaulow, H., Damgard-Jensen, A.D., Chatterji S. (1979), *Structural
483 and ingredient analysis of concrete – methods, results and experience*, Nordisk Betong, Vol. 3, 4-9.
- 484 [8] Mayfield, B. (1990), The quantitative evaluation of the water/cement ratio using fluorescence
485 microscopy, *Mag. Concr. Res.*, Vol. 42 No.150, 45-49.
- 486 [9] Elsen, J., Lens, N., Aarre, T., Quenard, D., Smolej V. (1995), “Determination of the w/c ratio of
487 hardened cement paste and concrete samples on thin sections using automated image analysis
488 techniques, *Cem. Concr. Res.*, Vol. 25, No. 4, 827-834.
- 489 [10] Jakobsen, U.H., Laugesen, P., Thaulow, N. (1998), Determination of water-cement ratio in hardened
490 concrete by optical fluorescence microscopy, *Water-Cement Ratio and other Durability Parameters:
491 Techniques for determination*, M.S. Khan (ed.), SP 191-3, ACI International, Los Angeles, 27-41.
- 492 [11] Sahu, S., Badger, S., Thaulow, N., Lee, R.J. (2004), Determination of water-cement ratio of hardened
493 concrete by scanning electron microscopy, *Cem. Concr. Comp.*, Vol. 26, No. 8, 987-992.

- 494 [12] Taylor, H.F.W. (1997), *Cement Chemistry*, Second edition, Thomas Telford, London, 459p.
- 495 [13] Bentz, D.P. (1997), Three-dimensional computer simulation of Portland cement hydration and
496 microstructure development, *J. Am. Ceram. Soc.*, Vol. 80, No. 1, 3-21.
- 497 [14] Powers, T.C., Brownyard, T.L. (1946-1947), Studies of the physical properties of hardened Portland
498 cement paste, Bull. 22, Res. Lab. of Portland Cement Association, Skokie, IL, USA, reprinted from *J.*
499 *Am. Concr. Inst. (Proc.)* Vol 43 in 9 parts, pp. 101-132, 249-336, 469-504, 549-602, 669-712, 845-880,
500 933-992.
- 501 [15] Hansen, T.C. (1986), Physical structure of hardened cement paste. A classical approach, *Materials and*
502 *Structures*, Vol. 19, 423-436.
- 503 [16] Brouwers, H.J.H. (2004), The work of Powers and Brownyard revisited: Part 1, *Cem. Concr. Res.*, Vol.
504 34, 1697-1716.
- 505 [17] Brouwers, H.J.H. (2005), The work of Powers and Brownyard revisited: Part 2, *Cem. Concr. Res.*, Vol.
506 35, 1922-1936.
- 507 [18] O.M. Jensen, P.F. Hansen (2001), Water-entrained cement-based materials I. Principles and theoretical
508 background, *Cem. Concr. Res.*, 31, 647-654.
- 509 [19] Scrivener, K.L. (2004), Backscattered electron imaging of cementitious microstructures: understanding
510 and quantification, *Cem. Concr. Comp.*, Vol. 26, No. 8, 935-945.
- 511 [20] Goldstein, J., Newbury, D., Joy, D., Lyman, C., Echlin, P., Lifshin, E., Sawyer, L., Michael, J. (2003),
512 *Scanning Electron Microscopy and X-Ray Microanalysis*, Third Edition, Kluwer Academic/Plenum
513 Publishers, New York, 689p.
- 514 [21] Taylor, H.F.W. (1989), Modification of the Bogue Calculation, *Adv. Cem. Res.*, Vol. 2, No. 6, 73-77.
- 515 [22] Wong, H.S., Buenfeld, N.R. (2006), Patch microstructure in cement-based materials: Fact or artefact?,
516 *Cem. Concr. Res.*, Vol. 36, No. 5, 990-997.
- 517 [23] Underwood, E.E. (1970), *Quantitative Stereology*, Addison-Wesley, Reading, Massachusetts, 274p.
- 518 [24] Wong, H.S., Head, M.K., Buenfeld, N.R. (2006), Pore segmentation of cement-based materials from
519 backscattered electron images, *Cem. Concr. Res.*, Vol. 36, No. 6, 1083-1090.

- 520 [25] X. Feng, E.J. Garboczi, D.P. Bentz, P.E. Stutzman, T.O. Mason (2004), Estimation of the degree of
521 hydration of blended cement pastes by a scanning electron microscope point-count procedure, *Cem.*
522 *Concr. Res.*, 34 [10] 1787-1793.